An adaptive minimum-maximum value-based weighted median filter for removing high density salt and pepper noise in medical images

Bharat Garg

Thapar Institute of Engineering and Technology Patiala,
Punjab, India
Email: bharat.garg@thapar.edu

Abstract: This paper presents an adaptive minimum-maximum value-based weighted median (AMMWM) filter that effectively restores noisy pixel in medical images at high noise density. The proposed filter computes two highly correlated groups of noise-free pixels using minimum and maximum value of the current window. Further, weighted medians of these groups determine the estimated value of candidate noisy pixel. If the current window fails to provide any noise-free pixels, its size is increased by one. The maximum size of window considered is 7×7 to minimise blurring. The proposed AMMWM filter is evaluated on various medical images where it provides higher quality metrics while preserving image features even at higher noise density. The simulation results using X-ray images show on an average 0.3 dB and 3.56 dB higher value of PSNR for wide (10%–90%) and very high (91%–98%) noise density ranges respectively.

Keywords: salt-and-pepper noise; median filter; mean filter; nonlinear filter; image processing.

Reference to this paper should be made as follows: Garg, B. (xxxx) 'An adaptive minimum-maximum value-based weighted median filter for removing high density salt and pepper noise in medical images', *Int. J. Ad Hoc and Ubiquitous Computing*, Vol. x, No. x, pp.xxx–xxx.

Biographical notes: Bharat Garg received his BE in Electronics from the Rajiv Gandhi Technical University, Bhopal, in 2001, and MTech in VLSI Design and PhD from the ABV-Indian Institute of Information Technology and Management Gwalior, India, in 2007, and 2017 respectively. He is currently working as an Assistant Professor in the Electronics and Communication Engineering Department in Thapar Institute of Engineering and Technology, Patiala. His research interest includes design and development of energy efficient VLSI architectures and hardware security. He has authored/co-authored more than 30 research papers in peer reviewed international Journals and conferences.

1 Introduction

Last three decades show significant improvement in medical imaging for diagnosing diseases at various stages. The availability of sophisticated technology such as ultrasonography, computed tomography and medical resonance imaging (MRI) made it possible to detect diseases at early stages with no pain to the patients (Brahme, 2014). There are different techniques used to capture images in different devices where error/fault may introduce noise in the captured images. SAP is the noise where corrupted pixels attain maximum (salt) or minimum (pepper) value (Gonzalez and Rafael, 2002). Under high noise density, the corrupted image completely losses image information and exhibits poor visual quality. Therefore, the resulting noisy image fails to provide information during diagnosis. The nonlinear median filtering is the preferred technique for SAP noise removal and to retrieve the images with clarity of subtle features and high visual quality (Astola and Kuosmaneen, 1997; Pitas and Venetsanopoulos, 2013). In median filter (MF), the median of pixels of selected window is used restore the corrupted pixel. The filter has the advantage of utilising original neighbouring pixels for computing the value of corrupted pixels. However, it is ineffective at low noise density ranges as most of the processed pixels attain extreme values at high noise density.

To enhance the quality of filtered image at medium and high noise density, various filters are presented. The switching MF detects noisy pixels and computes median of corrupted pixels only (Zhang and Karim, 2002; Ng and Ma, 2006). At high noise density, SMF also fails to retrieve median as noise-free pixel (NFP) since all pixels of the current window are noisy. Therefore, adaptive median filter (AMF) is presented in Hwang and Haddad (1995) that increases the window size with increasing noise density. However, consideration of large window size under high noise density condition causes

significant loss in edge information and AMF provides blurred images. To address this issue, a decision-based MF is presented where noisy pixel is restored by either the median of non-noisy pixels or nearest original pixel (Srinivasan and Ebenezer, 2007). However, this filter also provides images with streaking effect at high noise density. Therefore, several adaptive switching (Esakkirajan et al., 2011; Li et al., 2014; Arora et al., 2018; Ramachandran and Kishorebabu, 2019; Murugan et al., 2019) and fuzzy logic-based (Ahmed and Das, 2013) filters are presented to recover the image without blurring and streaking effect while exhibiting required edge details. However, recent fuzzy logic-based filters are able to eliminate noise at high noise density. But they still show poor edge information. Therefore, in this paper, a novel adaptive minimum-maximum value-based weighted median (AMMWM) filter is proposed. The proposed filter provides superior image quality in comparison to the existing median filters.

The paper is organised as follows. Section 2 provides related work whereas Section 3 presents proposed filter's flowchart, algorithm and an illustration using an example. Section 4 presents simulation results and analysis whereas Section 5 concludes the paper.

2 Related work

The medical imaging has seen significant improvement in recent years with sophisticated devices able to detect/diagnose tumours, fractures, cysts, etc. The SAP noise may occur during image capturing, storage or transmission due to fault in camera sensor, memory or noisy channel respectively. In the literature, various filtering techniques such as the mean/median, interpolation and weighted mean are presented to remove SAP noise while maintaining the image contents. The SMF is effective at low and medium noise density ranges as most of the processed pixels can attain noise-free values (Pitas and Venetsanopoulos, 2013). At higher noise density, SMF fails to retrieve median as non-extreme pixel even with large window size where blurring effect starts dominating. Therefore, decision-based median filter (DBAMF) is presented in Srinivasan and Ebenezer (2007) that tries to reduce the above-mentioned problem by making specific decisions (pixel is noisy or noisy-free) in 3×3 window. If noisy, pixels of this window are sorted row, columns and right diagonally. The central pixel of this sorted window is taken as median value. However, if the median is still noisy then the nearest NFP is used for replacement. The prime issue of this filter is that when the entire window is corrupted, previous pixel is repeated which may lead to blurring and loss of edge information.

To improve the performance, new filters like unsymmetric trimmed MF (UTMF) (Aiswarya et al., 2010) and unsymmetric trimmed midpoint filter (UTMP) are appended to the DBAMF. The UTMF provides better performance on lower noise density, whereas UTMP works well on high noise density. Both algorithms consider a 3×3 window across the noisy pixel and replace candidate pixel either by mean or mid-point of window using UTMF or UTMP respectively based on noise density. Further, a MDBUTM filter is presented in Esakkirajan et al. (2011) that estimates the median of noise-free pixels of 3×3 window to restore the candidate noisy pixel. However, under the conditions where all pixels in the considered window are corrupted, mean of all pixels of selected window is used as an alternative. It is this alternate value that results in poor image quality. The decision-based coupled window MF (DBCWMF) (Bhadouria et al., 2014) replaces corrupted pixel by the median of all uncorrupted pixels of 3×3 window centred on the candidate noisy pixel. In the case where none of pixels of the current window are found to be uncorrupted, its size is increased symmetrically. The maximum window size extension is limited to 9×9 to reduce blurring. If all pixels of this maximum sized window are noisy, then mean of this window restores the noisy pixels. The use of variable window sizes for median calculation is a better alternative than using the mean of a 3×3 window. Therefore, DCBWMF performs better than MDBUTM filter. However, the use of very large window sizes (7×7 and 9×9) under high noise density conditions causes blurred output image.

The FSBMM filter (Vijaykumar et al., 2014) utilises combination of mean and MFs to estimate the value of noisy pixel. In this filter, mean of previously processed pixels restores the noisy pixel when current window does not have any uncorrupted pixel otherwise; median of the non-extreme pixels restores the noisy pixel. Further, in the FSBMM, noisy pixels on the boundary are replaced by the previously proposed pixels in their respective row/column when these boundary pixels cannot be denoised using median. Therefore, at high noise density, the filtered images have repetition of pixels at the boundary which result in poor image quality. Further, the recursive spline interpolation filter (RSIF) presented in Veerakumar et al. (2014) utilises cubic spline interpolation for estimating the value of noisy pixel and showed better estimation at low to median range of noise density. Since RSIF requires at least two non-extreme pixels for interpolation which are rarely available at very high noise density ($\geq$90%), it does not to estimate fairly good pixels value at such high noise density.

Adaptive switching weighted MF (Faragallah and Ibrahem, 2016) has two stages namely noise detection followed by denoising. In noise detection stage, a pixel with value 255 (0) is considered as noisy if the mean value of the current window is not nearly equals to 255 (0); otherwise pixel is considered as noise-free. At the second stage, number of non-extreme pixels in the selected window is checked and if found odd, the median of non-extreme pixels is calculated to restore noisy pixel. Otherwise, the median of the window is calculated after repeating the most repeated value or the nearest non-corrupted value (when most repeated value is not available). It is often observed that the entire 3×3 window is corrupted at high noise density, therefore, under this condition the window size is increased to 5×5 and similar steps as before

are performed. The use of nearest uncorrupted pixel for median calculation essentially results in substitution of the corrupted pixel by the same nearest non-noisy pixel. This is one of the major drawbacks as it results in streaking under high noise density conditions.

A DAMF presented in Erkan et al. (2018) does symmetric padding instead of zero padding and first creates binary image from the noisy input image. All 0's and 255's are replaced by 0 while all other values are replaced by 1. Based on the values in the binary matrix, the median of 3 × 3 window centred on the noisy pixel is computed as denoised value. If the window exhibits noisy pixels only then its size is increased till at least one non-noisy value is encountered where median of uncorrupted values is used for substitution. However, the window size is limited to 7 × 7. Once processing is completed, the corrupted pixel in the output image (pixels left corrupted in the first stage) is restored by the median values of the 3 × 3 window. The three-valued weighted approach (TVWA) (Lu et al., 2016) considers a 3 × 3 window across the corrupted pixel and then divides all non-noisy pixels of this window into three groups based on their correlation with the middle, minimum and maximum pixel values. The lengths of these groups determine their weight. The corrupted pixel is restored by the weighted mean. When the selected 3 × 3 window is completely corrupted, its size is increased to 5 × 5 and the same process as before is repeated. The window size is increased to a maximum of 7 × 7. The major problem with the filter is its use of large window sizes resulting in blurred output images. Further, consideration of maximum, minimum and middle values in place of median value in pixel estimation reduces its closeness with the original pixel.

The next section presents proposed AMMWM algorithm that optimally denoises noisy pixel even at very high noise density.

3 Proposed AMMWM filtering approach

The image denoising has become a necessary step in MRI and CT scan imaging processes to evacuate undesirable noisy component. An effective denoising technique is required to sustain the stability among two components which are noise removal and preservation of image features. The proposed algorithm not only replaces each noisy pixel with optimal value but also maintains the original edge information of the image. This section first presents preliminaries, followed by flowchart and algorithm of the proposed approach and finally presents an example under different noise density.

3.1 Preliminaries

This subsection first presents basic terminologies used in the proposed algorithm.

3.1.1 Noise model

Two extreme values of a pixel, 255 and 0 representing salt and pepper respectively are considered as noisy. A noise vector (γ) containing these extreme pixels is considered.

$$\gamma = [0, 255] \tag{1}$$

where probability of each element is equal. In the proposed algorithm, each pixel is detected as either noisy ($P_{i,j} \in \gamma$) or noise-free ($P_{i,j} \notin \gamma$). The filtering process is applied for noisy pixels while the noise-free pixels left unchanged.

3.1.2 Window size selection

To reduce blurring and estimating optimal value of noisy pixel from the nearest neighbours, the proposed algorithm initially considers a small window $w^n_{(2\kappa+1)\times(\kappa+1)}$ with window size parameter (κ) equals to 1. If none of pixels of the considered window are noise-free, the κ is increased by one ($\kappa = \kappa + 1$). The maximum value of κ considered in the proposed algorithm is 3 as the blurring in filtered image increases with window size.

Figure 1 Flowchart of the proposed AMMWM algorithm (see online version for colours)

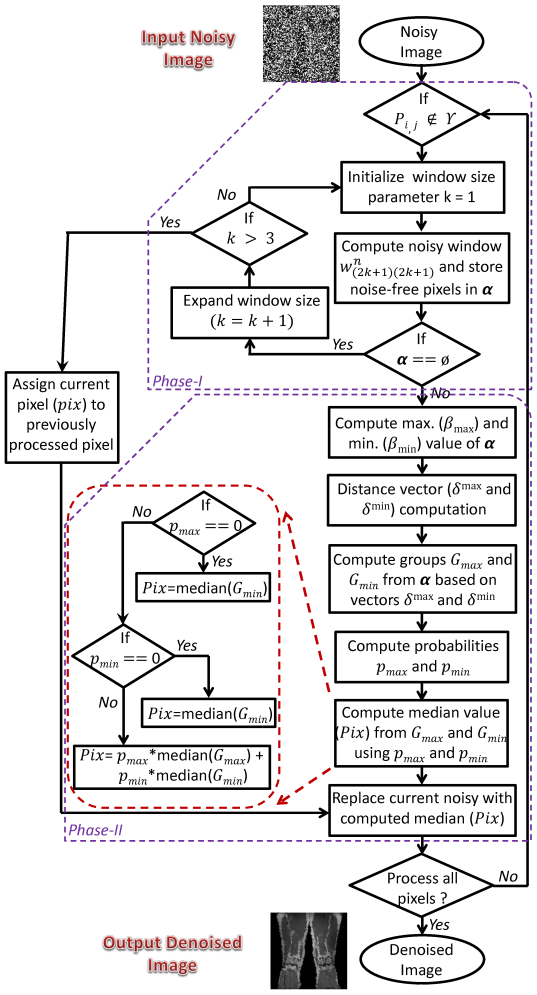

Algorithm 1 AMMWM (Img^n, Img^{nf}) (see online version for colours)

Input Img^n ▷ *Input noisy image*
Output Img^{nf} ▷ *Output filtered image*
for each $iP^n_{i,j} \in Img^n$ **do**
  Initialise: $\gamma = [0, 255]$; ▷ *Set of noisy pixels*
  Initialise: $\kappa \leftarrow 1$; ▷ *window size parameter*
  Compute $w^n_{(2\kappa+1)\times(\kappa+1)}$ centred at $iP^n_{i,j}$.
  for each $w^n_{l,m} \notin \gamma$ **do**
    Compute $\alpha \leftarrow [\alpha, w^n_{l,m}]$; ▷ *$\alpha$ stores NEP of $w^n_{l,m}$*
  end for
  $\eta^\alpha \leftarrow$length(α); ▷ *Number of NEP*
  if $\eta^\alpha \neq 0$ **then**
    $Pix \leftarrow$ TVL(α);
  else
    $\kappa \leftarrow \kappa + 1$;
    if $\kappa < 4$ **then** ▷ *Limit window size to 7 × 7*
      goto Line number 5.
    end if
  end if
  $Img^{nf}_{i,j} \leftarrow pix$;
end for
Return Img^f;
End ▷ *End of the algorithm*
Procedure: TVL(α) ▷ *TVL procedure*
$\beta_{\max} \leftarrow \max(\alpha)$; ▷ *Maximum value of α*
$\beta_{\min} \leftarrow \min(\alpha)$;
$\delta^{\max} \leftarrow |\beta_{\max} - \alpha|$; ▷ *Absolute difference between maximum value and each element of α_i*
$\delta^{\min} \leftarrow |\beta_{\min} - \alpha|$;
$G_{\max} \leftarrow \phi$, $G_{\min} \leftarrow \phi$; ▷ *Initialise $G_{\max}$*
for each α_i **do**
  if $\delta^{\max}_i \leq \delta^{\min}_i$ **then** ▷ *Check closeness of α_i to $G_{\max}$/$G_{\min}$*
    $G_{\max} \leftarrow [G_{\max}, \alpha_i]$; ▷ *Store α_i in $G_{\max}$*
  else
    $G_{\min} \leftarrow [G_{\min}, \alpha_i]$;
  end if
end for
$\eta_{\max} \leftarrow$length($G_{\max}$); ▷ *Number of NEP in $G_{\max}$*
$\eta_{\min} \leftarrow$length($G_{\min}$);
$P_{\max} \leftarrow \eta_{\max}/\eta_\alpha$; ▷ *Probability of NEP in $G_{\max}$*
$P_{\min} \leftarrow \eta_{\min}/\eta_\alpha$;
if $P_{\max} == 0$ **then**
  $pix \leftarrow$median($G_{\min}$); ▷ *Compute median of $G_{\min}$*
else if $P_{\min} == 0$ **then**
  $pix \leftarrow$median($G_{\max}$);
else
  $pix \leftarrow P_{\max}$*median($G_{\max}$) + $P_{\min}$*median($G_{\min}$);
end if
Return Pix;

3.1.3 Minimum and maximum group computation

In the proposed algorithm, the non-extreme pixels of the current window are stored in an array (α) and then minimum ($\beta_{\min}$) and maximum ($\beta_{\max}$) values of this array are calculated. Further, two groups namely minimum and maximum ($G_{\min}$ and $G_{\max}$) are created correspond to $\beta_{\min}$ and $\beta_{\max}$ respectively of the selected window. Finally, each pixel of the α is assigned to either $G_{\min}$ or $G_{\max}$ based on the closeness to $\beta_{\min}$ or $\beta_{\max}$ respectively. These groups are used to estimate the noisy pixel value in the proposed algorithm. The next subsection presents the flowchart of the proposed algorithm.

Figure 2 Illustration of proposed AMMWM filtering algorithm (see online version for colours)

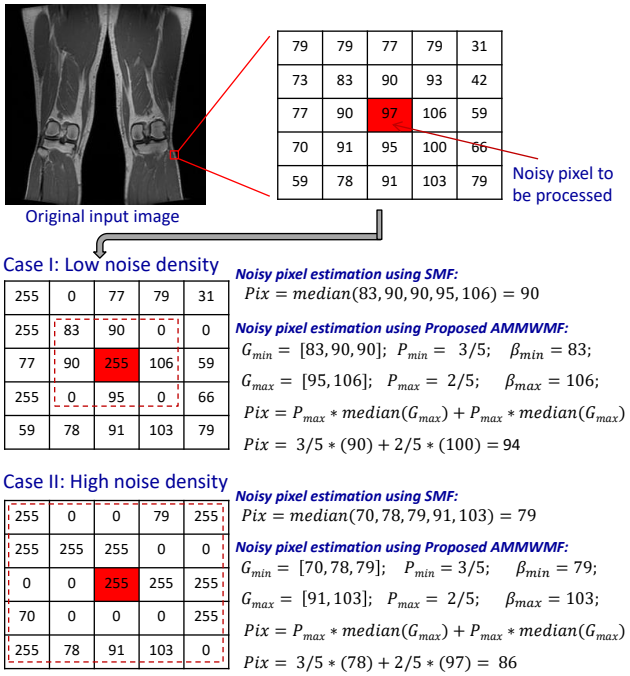

3.2 Proposed AMMWM filter flowchart

The flowchart of proposed filter is shown in Figure 1. It first identifies whether the candidate pixel is noisy or noise-free. For each noisy pixel, an appropriate window (such that it exhibits at least one non-extreme pixel) around the noisy pixel is selected. If this window exhibits noisy pixels only, its size is increased by one. The maximum size of the window that is considered in the proposed approach is 7 × 7. To estimate the effective value of noisy pixel, only non-extreme pixels are considered which are stored in an array (α). The initial steps used to compute appropriate size of window is encircled with dotted line ($Phase - I$) in Figure 1.

The output (α) of $Phase\text{-}I$ is given to $Phase\text{-}II$ where the $\beta_{\max}$ and $\beta_{\min}$ are first computed from α and then distance vector (δ) corresponds to the $\beta_{\max}$ and $\beta_{\min}$ are calculated ($\delta^{\max} = \alpha - \beta_{\max}$, $\delta^{\min} = \alpha - \beta_{\min}$). With the help of $\delta^{\max}$ and $\delta^{\min}$, two groups $G_{\max}$ and $G_{\min}$ are created. The pixels of α which are more closer to maximum ($\delta^{\max} \leq \delta^{\min}$) are added to $G_{\max}$, otherwise they are added to $G_{\min}$. Further, the weight/probability of each group ($P_{\max} = length(G_{\max})/length(\alpha)$ and $P_{\min} = length(G_{\min})/length(\alpha)$) is computed. Finally, the noisy pixel is restored by the value (Pix) obtained via median and probability of each group using equation (2).

$$Pix = P_{\max} \star median(G_{\max}) + P_{\min} \star median(G_{\min}) \quad (2)$$

Table 1 PSNR and SSIM of proposed and existing SAP removal techniques for thigh images with varying noise density (10%–90%)

Metrics	*Noise density (%)*	*SMF (Astola and Kuosmaneen, 1997)*	*DBAMF (Srinivasan and Ebenezer, 2007)*	*ITSAMFT (Deivalakshmi and Palanisamy, 2010)*	*MDBUTM (Esakkirajan et al., 2011)*	*FSBMM (Vijaykumar et al., 2014)*
PSNR (dB)	10	38.68	33.84	30.83	30.45	36.78
	20	30.42	32.13	32.57	27.84	33.48
	30	24.15	29.27	31.65	25.59	31.01
	40	19.14	27.77	29.90	23.84	29.15
	50	15.01	26.22	28.36	21.42	27.93
	60	12.26	23.79	26.38	19.30	26.82
	70	9.60	21.50	24.12	16.75	25.74
	80	7.50	19.71	21.77	14.10	24.34
	90	5.74	16.88	17.62	11.12	22.47
	Avg	*18.06*	*25.68*	*27.02*	*21.16*	*28.64*
SSIM	10	0.9890	0.9760	0.9596	0.9083	0.9790
	20	0.9500	0.9595	0.9654	0.8769	0.9640
	30	0.8365	0.9346	0.9510	0.8367	0.9420
	40	0.6201	0.9004	0.9235	0.7854	0.9183
	50	0.3586	0.8608	0.8851	0.7055	0.8915
	60	0.2018	0.8012	0.8257	0.5953	0.8612
	70	0.0898	0.7124	0.7391	0.4412	0.8226
	80	0.0390	0.6076	0.6320	0.2722	0.7648
	90	0.0165	0.4195	0.4756	0.1302	0.6537
	Avg	*0.4557*	*0.7969*	*0.8174*	*0.6169*	*0.8663*

Metrics	*RSIF (Veerakumar et al., 2014)*	*PBDM (Balasubramanian et al., 2016)*	*DAMF (Erkan et al., 2018)*	*BPDM (Erkan and Gökrem, 2018)*	*TVWA (Lu et al., 2016)*	*Proposed*
PSNR (dB)	36.38	24.72	30.19	23.19	35.29	34.08
	33.67	19.40	27.47	20.07	33.08	32.78
	31.17	17.14	25.23	18.13	31.15	31.60
	29.26	15.36	23.55	16.86	29.69	30.31
	27.89	14.47	21.13	15.53	27.90	29.13
	25.99	14.09	19.01	14.89	26.46	27.84
	24.31	13.75	16.56	14.07	24.83	26.89
	22.36	13.85	13.98	13.47	22.73	25.24
	19.50	13.35	11.03	13.15	18.93	22.61
	27.84	*16.24*	*20.90*	*16.60*	*27.78*	*28.94*
SSIM	0.9775	0.8454	0.9083	0.6855	0.9749	0.9758
	0.9665	0.6004	0.8769	0.5767	0.9638	0.9665
	0.9494	0.4176	0.8367	0.5122	0.9510	0.9564
	0.9274	0.2983	0.7853	0.4705	0.9369	0.9426
	0.9038	0.2291	0.7054	0.4295	0.9178	0.9264
	0.8669	0.2028	0.5953	0.4062	0.8940	0.9052
	0.8126	0.1785	0.4412	0.3785	0.8585	0.8752
	0.7270	0.1719	0.2722	0.3438	0.7908	0.8232
	0.5657	0.1821	0.1302	0.3209	0.6065	0.7300
	0.8552	*0.3473*	*0.6168*	*0.4582*	*0.8771*	*0.9001*

Table 2 Quality metrics of proposed and existing SAP removal techniques using thigh image with very high noise density range (91%–98%)

Metrics	*Noise density (%)*	*SMF (Astola and Kuosmaneen, 1997)*	*DBAMF (Srinivasan and Ebenezer, 2007)*	*ITSAMFT (Deivalakshmi and Palanisamy, 2010)*	*MDBUTM (Esakkirajan et al., 2011)*	*FSBMM (Vijaykumar et al., 2014)*
PSNR (dB)	91	6.75	21.67	12.69	15.10	25.72
	92	6.63	21.55	12.04	14.75	25.57
	93	6.42	20.82	11.34	14.32	24.09
	94	6.32	20.43	10.67	14.19	23.09
	95	6.18	18.62	9.87	13.73	22.96
	96	6.00	17.92	9.22	13.41	21.78
	97	5.90	16.65	8.55	13.08	20.07
	98	5.75	15.41	7.69	12.73	17.56
	Avg	*6.24*	*19.13*	*10.26*	*13.91*	*22.61*

Table 2 Quality metrics of proposed and existing SAP removal techniques using thigh image with very high noise density range (91%–98%) (continued)

Metrics	*Noise density (%)*	*SMF (Astola and Kuosmaneen, 1997)*	*DBAMF (Srinivasan and Ebenezer, 2007)*	*ITSAMFT (Deivalakshmi and Palanisamy, 2010)*	*MDBUTM (Esakkirajan et al., 2011)*	*FSBMM (Vijaykumar et al., 2014)*
SSIM	91	0.0080	0.5112	0.1999	0.1406	0.7019
	92	0.0068	0.4793	0.1734	0.1252	0.6926
	93	0.0082	0.4396	0.1560	0.1113	0.6694
	94	0.0063	0.4233	0.1379	0.1009	0.6537
	95	0.0065	0.3481	0.1095	0.0830	0.6271
	96	0.0050	0.3048	0.0978	0.0740	0.5988
	97	0.0054	0.2452	0.0743	0.0659	0.5636
	98	0.0039	0.1788	0.0530	0.0517	0.5110
	Avg	*0.0063*	*0.3663*	*0.1252*	*0.0941*	*0.6273*
Metrics	*RSIF (Veerakumar et al., 2014)*	*PBDM (Balasubramanian et al., 2016)*	*DAMF (Erkan et al., 2018)*	*BPDM (Erkan and Gökrem, 2018)*	*TVWA (Lu et al., 2016)*	*Proposed*
PSNR (dB)	22.23	9.13	15.02	10.74	22.32	28.28
	22.51	8.81	14.69	10.34	21.94	27.95
	21.89	8.51	14.26	10.15	21.31	27.48
	21.77	8.21	14.12	9.79	20.93	27.35
	21.17	7.83	13.67	9.38	20.17	26.47
	20.00	7.56	13.35	8.98	19.29	25.39
	18.92	7.22	13.05	8.56	18.36	23.75
	17.75	6.83	12.69	7.76	17.01	22.69
	20.78	*8.01*	*13.86*	*9.46*	*20.17*	*26.17*
SSIM	0.6506	0.0477	0.1405	0.0482	0.7498	0.7754
	0.6395	0.0426	0.1252	0.0444	0.7316	0.7631
	0.6110	0.0398	0.1113	0.0437	0.6815	0.7470
	0.6020	0.0396	0.1008	0.0384	0.6439	0.7256
	0.5636	0.0366	0.0830	0.0392	0.5656	0.6927
	0.5393	0.0353	0.0740	0.0360	0.4915	0.6519
	0.4898	0.0318	0.0659	0.0336	0.4272	0.6006
	0.4512	0.0256	0.0517	0.0279	0.3328	0.5381
	0.5684	*0.0374*	*0.0940*	*0.0389*	*0.5780*	*0.6868*

Table 3 PSNR and SSIM of proposed and existing SAP removal techniques for various medical images at 95% noise density

Metrics	*Benchmark images (%)*	*SMF (Astola and Kuosmaneen, 1997)*	*DBAMF (Srinivasan and Ebenezer, 2007)*	*ITSAMFT (Deivalakshmi and Palanisamy, 2010)*	*MDBUTM (Esakkirajan et al., 2011)*	*FSBMM (Vijaykumar et al., 2014)*
PSNR	Chest	6.18	18.62	9.87	13.73	22.96
	Abdomen	5.07	18.49	16.71	10.03	22.15
	Head	4.40	17.86	18.21	8.44	22.77
	Mammogram	2.98	22.97	11.30	6.45	28.83
	Retinal	4.02	21.54	11.76	10.63	26.86
	Average	*4.53*	*19.90*	*13.57*	*9.86*	*24.71*
SSIM	Chest	0.0065	0.3481	0.1095	0.0830	0.6271
	Abdomen	0.0087	0.2838	0.1886	0.0560	0.5315
	Head	0.0051	0.5087	0.5635	0.0384	0.6123
	Mammogram	0.0170	0.5461	0.5900	0.0948	0.6616
	Retinal	0.0079	0.6789	0.2357	0.0701	0.8109
	Average	*0.0090*	*0.4731*	*0.3374*	*0.0685*	*0.6487*
Metrics	*RSIF (Veerakumar et al., 2014)*	*PBDM (Balasubramanian et al., 2016)*	*DAMF (Erkan et al., 2018)*	*BPDM (Erkan and Gökrem, 2018)*	*TVWA (Lu et al., 2016)*	*Proposed*
PSNR	21.17	7.83	13.67	9.38	20.17	26.47
	20.49	14.33	9.94	12.20	17.54	22.36
	19.87	15.06	8.37	15.53	15.29	22.85

Table 3 PSNR and SSIM of proposed and existing SAP removal techniques for various medical images at 95% noise density (continued)

Metrics	*RSIF (Veerakumar et al., 2014)*	*PBDM (Balasubramanian et al., 2016)*	*DAMF (Erkan et al., 2018)*	*BPDM (Erkan and Gökrem, 2018)*	*TVWA (Lu et al., 2016)*	*Proposed*
PSNR	18.99	9.58	6.44	11.78	7.86	26.34
	23.93	7.86	10.56	8.62	24.38	28.31
	20.89	*10.93*	*9.80*	*11.50*	*17.05*	*25.27*
SSIM	0.5636	0.0366	0.0830	0.0392	0.5656	0.6927
	0.4586	0.0941	0.0559	0.0584	0.3874	0.5679
	0.5367	0.2956	0.0384	0.5128	0.3267	0.7058
	0.5401	0.5624	0.0948	0.5896	0.4649	0.6801
	0.7737	0.0654	0.0700	0.1016	0.7899	0.8444
	0.5746	*0.2108*	*0.0685*	*0.2603*	*0.5069*	*0.6982*

This procedure is executed to denoise all corrupted pixels. Further, if the maximum window (7×7) does not get even single non-extreme pixel, the previously processed pixel is considered as an alternative to replace the candidate noisy pixel. The next subsection presents proposed AMMWM algorithm.

3.3 Proposed AMMWM algorithm

The pseudo code of the proposed filter is given in Algorithm 1. It selects a small window around the noisy pixel and computes noise-free pixels of this window. If non-zero noise-free pixels are found, the algorithm estimates the value of noisy pixel by calling two valued logic (TVL) function (line number 23 to 47 of Algorithm 1) else the window size is increased. The maximum size of the window is considered is 7×7 as consideration of more size increases blurring effect. If maximum sized window fails to exhibit any noise-free pixel, the candidate noisy pixel is restored by the previously processed pixel (line number 19 of Algorithm 1). In the TVL function, two values of $\beta_{\max}$ and $\beta_{\min}$ from the current window are first calculated and then distance vectors $\delta^{\max}$ and $\delta^{\min}$ are calculated (line number 26 and 27). With the help of distance vector, group two groups $G_{\max}$ and $G_{\min}$ are computed. Each pixel of the current window is added to either $G_{\max}$ or $G_{\min}$ based on maximum or minimum value respectively (line number 29 to 35). Further, the length of each group is determined which is utilised to evaluate the probability of each group (e.g., $P_{\max} = \eta_{\max}/\eta_{\alpha}$) (line number 38 and 39). Finally, the weighted median of each group determines the estimated value of noisy pixel (line number 45). Since the proposed algorithm computes the median of two highly correlated groups, it provides median value more closer to the original pixel. Further, the consideration of weighted median increases the probability of estimated value close to original value of noisy pixel under processing. The next subsection presents an illustration of proposed algorithm.

3.4 Illustration of proposed algorithm

The estimation of denoised pixel using proposed algorithm with the help of example is demonstrated in Figure 2. An image segment of size 5×5 is considered and SAP noise with low and high density is introduced. The central corrupted pixel of this noisy segment is estimated using proposed and SMF (Astola and Kuosmaneen, 1997).

In case I with low noise density, small window of size 3×3 has few non-zero noise-free pixels, therefore, it is used to estimate value of denoised pixel. The proposed algorithm first calculates maximum ($\beta_{\max}$) and minimum ($\beta_{\min}$) value of this window after eliminating noisy pixels (α). Further, maximum and minimum groups ($G_{\max}$ and $G_{\min}$) are computed based on the closeness of each pixel of noise-free window to the $\beta_{\max}$ and $\beta_{\min}$ respectively. Further, the value of probability of each group ($P_{\max}$ and $P_{\min}$) are calculated. Finally, weighted median of both groups is used to restore the value of candidate noisy pixel. It can be observed from Figure 2 that the estimated value of noisy pixel using SMF and proposed method is 90 and 94 respectively. The value estimated using proposed algorithm come out to be closer to the original value (97) over the SMF.

In case II (at the higher noise density condition), 3×3 window fails to attain noise-free pixels, therefore, window size of 5×5 is considered where few non-extreme pixels are found. Using the same approach as above, the estimated value of median using SMF and proposed algorithm are 79 and 86 respectively.

Therefore, it can be observed that proposed filter estimates value closer to the original value even under high noise density condition. Thus, the proposed algorithm can be effectively utilised to eliminate the SAP noise at high noise density. The simulation results in the next section presents efficacy of the proposed algorithm over the existing SAP removal techniques.

4 Simulation results and analysis

The proposed AMMWM is analysed over the existing techniques namely SMF (Astola and Kuosmaneen, 1997), DBAMF (Srinivasan and Ebenezer, 2007), ITSAMFT (Deivalakshmi and Palanisamy, 2010), MDBUTM (Esakkirajan et al., 2011), FSBMM (Vijaykumar et al., 2014), RSIF (Veerakumar et al., 2014), PDBM (Balasubramanian et al., 2016), DAMF (Erkan et al., 2018), BPDM (Erkan and Gökrem, 2018) and TVWA (Lu et al.,

2016) using various medical images such as X-ray, MRI, Mammogram and retinal images. Initially, the SAP noise of varying noise density (wide range from 10% to 90% and very high noise density range from 91% to 98%) is introduced in these benchmark images and then resulting noisy images are filtered via proposed and existing filtering techniques and finally, the quality metrics are extracted. Both quantitative and qualitative analysis is done based on the extracted quality metrics and reconstructed images, respectively.

This section first presents various quality metrics considered for the quality analysis followed by the simulation results and analysis on low and high noise density.

4.1 Quality metrics

The quality metrics considered for the analysis are peak signal to noise ratio (PSNR) and structural similarity index (SSIM) (Wang et al., 2004). The PSNR in dB is given by

$$PSNR(db) = 10\log(I_{\max}^2/MSE) \tag{3}$$

where $I_{\max}^2$ and MSE are the maximum value of the signal and mean square error respectively. Whereas, the value of SSIM is given by

$$SSIM(x,y) = \frac{(2\mu_x\mu_y + C_1)(2\sigma_{xy} + C_2)}{(\mu_x^2 + \mu_y^2 + C_1)(\sigma_x^2 + \sigma_y^2 + C_2)} \tag{4}$$

where μ_x (σ_x) and μ_y (σ_y) represent mean (standard deviation) value in x and y directions, respectively. Further, C_1 and C_2 represent constants which are considered to limit the SSIM value to 1.

The next subsections present simulation results and analysis of X-ray images under varying noise density. Further, a comparative analysis on various other medical images under high noise density is presented.

4.2 Quality analysis on X-ray images for wide noise density

The thigh X-ray images (256 × 256) with 10% to 90% noise density are filtered via proposed and existing filters. The quality metrics are extracted and summarised in Table 1. These results show that the proposed AMMWM algorithm provides higher value of the PSNR and SSIM at each sample of noise density over the existing algorithms. On an average, the proposed filter provides 0.3 dB and 0.034 higher values of PSNR and SSIM, respectively over the best known algorithm (Vijaykumar et al., 2014). Further, it can be observed from Table 1 that the quality metrics, e.g., SSIM value of SMF, PDBM and BPDM decreases rapidly even when the noise density is smaller than 50% whereas, DAMF and ITSAMFT could provide acceptable value of SSIM up to 70% noise density. Whereas, the quality metrics of the proposed filter show high value of SSIM and PSNR for each sample of noise density and even at very high noise density (90%).

Finally, for qualitative analysis, the filtered X-ray images are shown in Figure 3. These images show that proposed filter recovers X-ray image of vary high perceptual quality even at high density (90%) over the others. However the images filtered via DBAMF, FSBMM, RSIF and FAHPF show good image quality; the proposed filter provides images with better edge information over all the existing.

The next subsection presents quality analysis on very high noise density ranges (91%–98%).

4.3 Analysis on very high noise density (91%–98%)

For quality analysis at very high noise density, Thigh images with 91% to 98% noise density are generated. These images are filtered via proposed and existing SAP removal techniques. The extracted quality metrics are summarised in Table 2. The values of the PSNR and SSIM of the proposed filter show higher quality of filtered images over the images recovered from the existing filters. Only four existing filters namely FSBMM, RSIF, DBAMF and TVWA could provide images with average PSNR value greater than 20 dB. Whereas, proposed filter an average provides 3.56 dB and 0.0595 higher values of PSNR and SSIM, respectively over the best known algorithm (Vijaykumar et al., 2014).

For comparative quality analysis, PSNR and SSIM for varying noise density are plotted as shown in Figure 4. From the figure it can be observed that proposed filter on higher noise density provides better value of PSNR and SSIM for each sample of noise density. Finally, for the qualitative analysis, the filtered images are extracted. These images show that proposed filter provides good images even at 97% noise density. However the visual quality of the images at 98% noise density is not so good but it provides image information of acceptable level.

4.4 Analysis on various medical images at 95% noise density

For the quality of the proposed algorithm on different medical images (X-ray, MRI, Mammogram and retinal images), the gray scaled chest (217 × 233), abdomen (256 × 256), head (256 × 256), mammogram (1,024 × 1,024) and coloured retinal (380 × 292) images are considered (Hall, n.d.; http://peipa.essex.ac.uk/info/mias.html). The SAP noise with 95% noise density is first introduced and the resulting noisy images are filtered via proposed and existing SAP removal techniques. The extracted quality metrics are summarised in Table 3. The value of the PSNR and SSIM of images filtered via proposed filter shows higher quality over the images recovered from the existing filters for each medical image. The proposed filter an average provides 0.56 dB and 0.0495 higher values of PSNR and SSIM, respectively over the best known algorithm (Vijaykumar et al., 2014). Finally, the extracted filtered images are shown Figure 5 where the proposed filter shows images with higher visual quality over the images filtered via existing filters.

Figure 3 Thigh images (256 × 256) with increasing noise density (10% to 90% from column left to right) filtered using, (a) SMF (b) DBAMF (c) ITSAMFT (d) MDBUTM (e) FSBMM (f) RSIF (g) PDBM (h) DAMF (i) BPDM (j) TVWA (k) proposed MFs

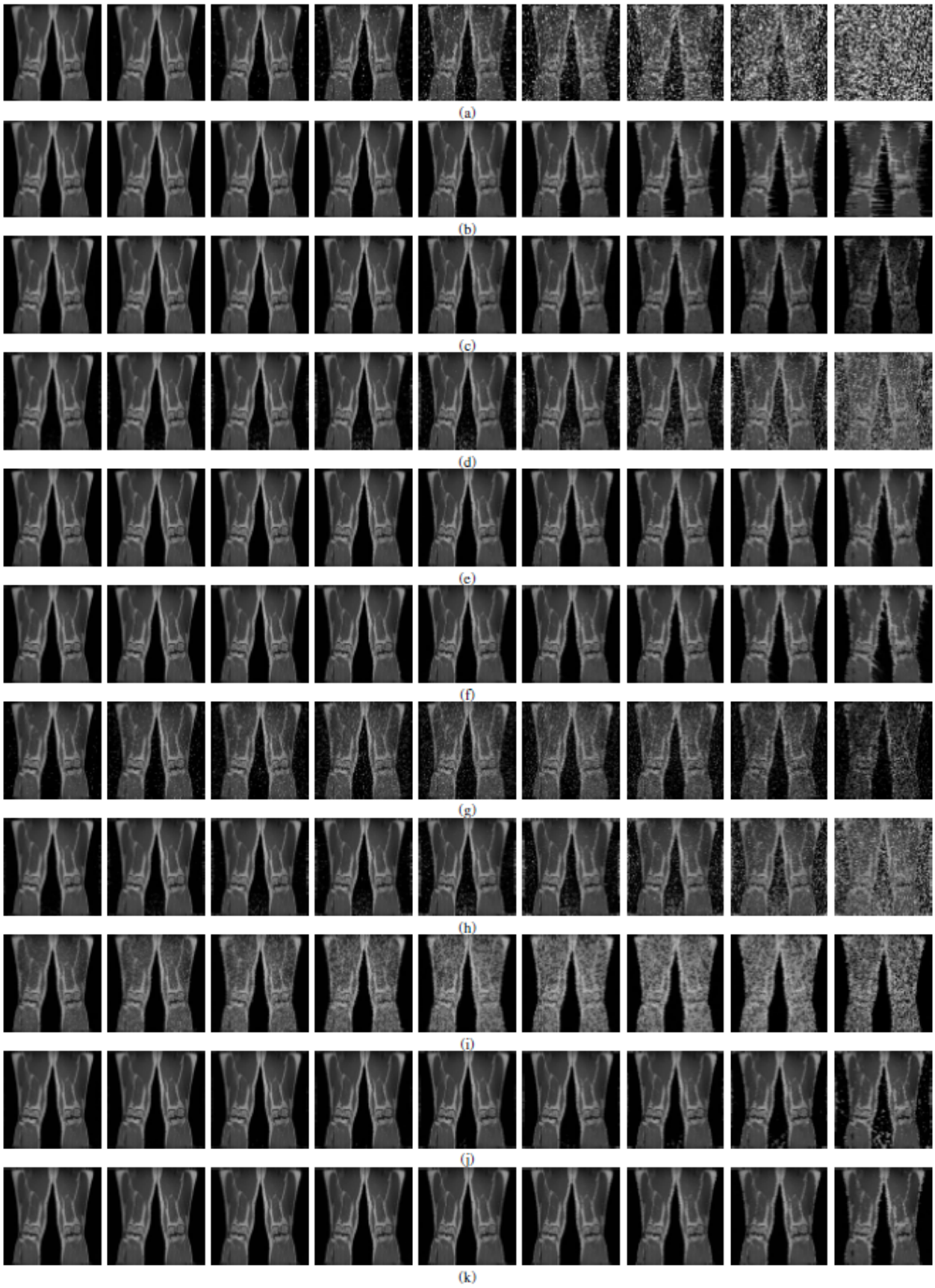

Figure 4 Quality metrics, (a) PSNR (b) SSIM comparison of thigh images filtered via proposed and existing filter with noise density from 91% to 98% (see online version for colours)

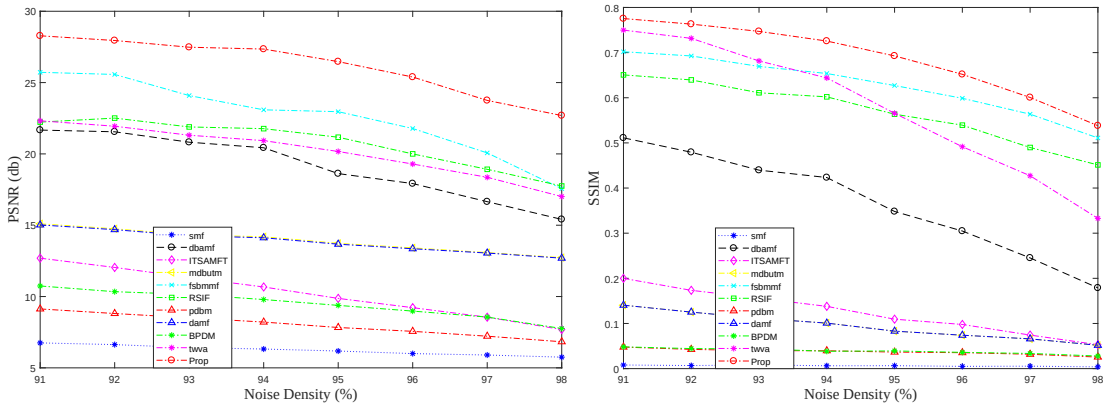

(a) (b)

Figure 5 Various coloured medical images, (a) original noise-free and images with 95% noise density filtered using, (b) SMF (c) DBAMF (d) ITSAMFT (e) MDBUTM (f) FSBMM (g) RSIF (h) PDBM (i) DAMF (j) BPDM (k) TVWA (l) proposed MFs (see online version for colours)

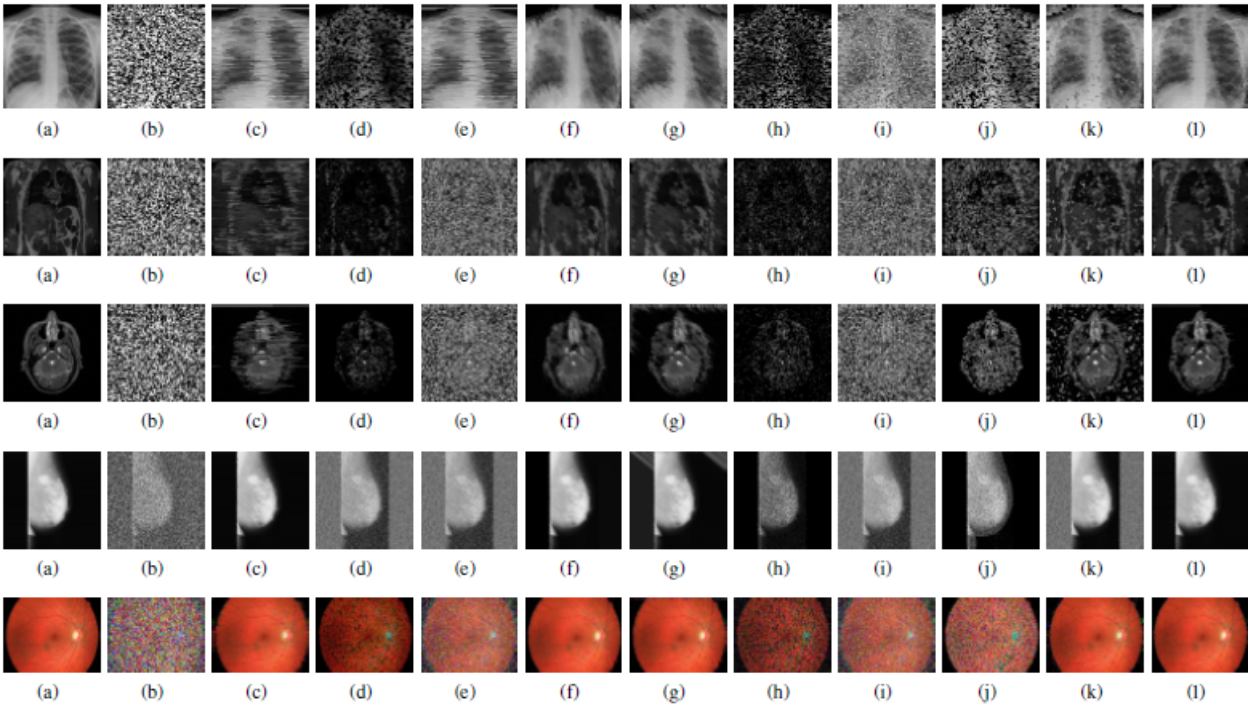

From the simulation results it can be observed that proposed filter effectively denoises the SAP noise while providing images with higher visual quality without significant loss of image features. Therefore, it can be effectively utilised for denoising medical images corrupted with salt and pepper noise.

5 Conclusions

This paper presented a novel adaptive minimum maximum value-based weighted MF that effectively denoise image while preserving image feature at high noise density. The proposed filter considers sliding window of adaptive size and computes array of noise-free pixels. If this array is empty, size of the window is increase. Two groups correspond to the minimum and maximum values of this noise-free pixels array are computed based on their closeness. Further weighted median of these groups provides estimated the value of noisy pixels. The proposed algorithm shows very high quality denoised image even at higher noise density. The quality analysis on medical images (X-ray thigh image) shows that proposed filter on an average provides 0.3 dB and 0.034 higher values of PSNR and SSIM, respectively for wide noise density range (10%–90%) whereas it provides 3.56 dB and 0.0595 higher values of PSNR and SSIM, respectively for very high noise density range (91%–98%) over the best known algorithm.

References

[online] http://peipa.essex.ac.uk/info/mias.html (accessed July 2019).

Ahmed, F. and Das, S. (2013) 'Removal of high-density salt-and-pepper noise in images with an iterative adaptive fuzzy filter using alpha-trimmed mean', *IEEE Transactions on Fuzzy Systems*, Vol. 22, No. 5, pp.1352–1358.

Aiswarya, K., Jayaraj, V. and Ebenezer, D. (2010) 'A new and efficient algorithm for the removal of high density salt and pepper noise in images and videos', in *2010 Second International Conference on Computer Modeling and Simulation*, IEEE, Vol. 4, pp.409–413.

Arora, S., Hanmandlu, M. and Gupta, G. (2018) 'Filtering impulse noise in medical images using information sets', *Pattern Recognition Letters*.

Astola, J. and Kuosmaneen, P. (1997) *Fundamentals of Nonlinear Digital Filtering*, CRC, Boca Raton, FL.

Balasubramanian, G., Chilambuchelvan, A., Vijayan, S. and Gowrison, G. (2016) 'Probabilistic decision based filter to remove impulse noise using patch else trimmed median', *AEU-International Journal of Electronics and Communications*, Vol. 70, No. 4, pp.471–481.

Bhadouria, V.S., Ghoshal, D. and Siddiqi, A.H. (2014) 'A new approach for high density saturated impulse noise removal using decision-based coupled window median filter', *Signal, Image and Video Processing*, Vol. 8, No. 1, pp.71–84.

Brahme, A. (2014) *Comprehensive Biomedical Physics*, Newnes, UK.

Deivalakshmi, S. and Palanisamy, P. (2010) 'Improved tolerance based selective arithmetic mean filter for detection and removal of impulse noise', in *2010 5th International Conference on Industrial and Information Systems*, IEEE, pp.309–313.

Erkan, U. and Gökrem, L. (2018) 'A new method based on pixel density in salt and pepper noise removal', *Turkish Journal of Electrical Engineering & Computer Sciences*, Vol. 26, No. 1, pp.162–171.

Erkan, U., Gökrem, L. and Enginoğlu, S. (2018) 'Different applied median filter in salt and pepper noise', *Computers & Electrical Engineering*, Vol. 70, pp.789–798.

Esakkirajan, S., Veerakumar, T., Subramanyam, A.N. and PremChand, C. (2011) 'Removal of high density salt and pepper noise through modified decision based unsymmetric trimmed median filter', *IEEE Signal Processing Letters*, Vol. 18, No. 5, pp.287–290.

Faragallah, O.S. and Ibrahem, H.M. (2016) 'Adaptive switching weighted median filter framework for suppressing salt-and-pepper noise', *AEU-International Journal of Electronics and Communications*, Vol. 70, No. 8, pp.1034–1040.

Gonzalez, W.R.E. and Rafael, C. (2002) *Digital Image Processing*, 2nd ed., Prentice Hall, New Jersey.

Hall, J. (n.d.) *Brain MRI Images* [online] http://overcode.yak.net/15 (accessed July 2019).

Hwang, H. and Haddad, R.A. (1995) 'Adaptive median filters: new algorithms and results', *IEEE Transactions on Image Processing*, Vol. 4, No. 4, pp.499–502.

Li, Z., Liu, G., Xu, Y. and Cheng, Y. (2014) 'Modified directional weighted filter for removal of salt & pepper noise', *Pattern Recognition Letters*, Vol. 40, pp.113–120.

Lu, C-T., Chen, Y-Y., Wang, L-L. and Chang, C-F. (2016) 'Removal of salt-and-pepper noise in corrupted image using three-values-weighted approach with variable-size window', *Pattern Recognition Letters*, Vol. 80, pp.188–199.

Murugan, K., Arunachalam, V. and Karthik, S. (2019) 'Hybrid filtering approach for retrieval of MRI image', *Journal of Medical Systems*, Vol. 43, No. 1, p.9.

Ng, P-E. and Ma, K-K. (2006) 'A switching median filter with boundary discriminative noise detection for extremely corrupted images', *IEEE Transactions on Image Processing*, Vol. 15, No. 6, pp.1506–1516.

Pitas, I. and Venetsanopoulos, A.N. (2013) *Nonlinear Digital Filters: Principles and Applications*, Vol. 84, Springer Science & Business Media, New York.

Ramachandran, V. and Kishorebabu, V. (2019) 'A tri-state filter for the removal of salt and pepper noise in mammogram images', *Journal of Medical Systems*, Vol. 43, No. 2, p.40.

Srinivasan, K. and Ebenezer, D. (2007) 'A new fast and efficient decision-based algorithm for removal of high-density impulse noises', *IEEE Signal Processing Letters*, Vol. 14, No. 3, pp.189–192.

Veerakumar, T., Esakkirajan, S. and Vennila, I. (2014) 'Recursive cubic spline interpolation filter approach for the removal of high density salt-and-pepper noise', *Signal, Image and Video Processing*, Vol. 8, No. 1, pp.159–168.

Vijaykumar, V., Mari, G.S. and Ebenezer, D. (2014) 'Fast switching based median-mean filter for high density salt and pepper noise removal', *AEU-International Journal of Electronics and Communications*, Vol. 68, No. 12, pp.1145–1155.

Wang, Z., Bovik, A.C., Sheikh, H.R., Simoncelli, E.P. et al. (2004) 'Image quality assessment: from error visibility to structural similarity', *IEEE Transactions on Image Processing*, Vol. 13, No. 4, pp.600–612.

Zhang, S. and Karim, M.A. (2002) 'A new impulse detector for switching median filters', *IEEE Signal Processing Letters*, Vol. 9, No. 11, pp.360–363.

Abbreviations

SAP	Salt and pepper
SMF	Switching median filter
ITSAMF	Improved tolerance-based selective arithmetic mean filtering
MDBUTM	Modified decision-based unsymmetrical trimmed median
FSBMM	Fast switching-based median mean
PDBM	Probabilistic decision-based median
DAMF	Different applied median filter
BPDM	Based on pixel density median
TVWA	Three value weighted approach

List of symbols

Img^n	Input noisy image
Img^{nf}	Output denoised Image
$iP^n_{i,j}$	Input noisy pixel located at i, j position
κ	Window size parameter
$w^n_{(\kappa+1)\times(\kappa+1)}$	Noisy window of $(\kappa+1)\times(\kappa+1)$ size
γ	Noise vector
α	Vector containing noise-free pixels of current window
$\beta_{\max}$	Maximum value of α
$G_{\max}$	Noise-free pixels of α more closer to $\beta_{\max}$ than $\beta_{\min}$
$\eta_{\max}$	Length of $G_{\max}$
$P_{\max}$	Weighting factor (length($G_{\max}$)/Length(α))